Science Advances
AAAS

Supplementary Materials for

Lattice strain modulation toward efficient blue perovskite light-emitting diodes

Baoxing Liu *et al.*

Corresponding author: Pu Huang, arvin_huang@szu.edu.cn; Tingchao He, tche@szu.edu.cn; Guijun Li, gliad@connect.ust.hk

Sci. Adv. **8**, eabq0138 (2022)
DOI: 10.1126/sciadv.abq0138

This PDF file includes:

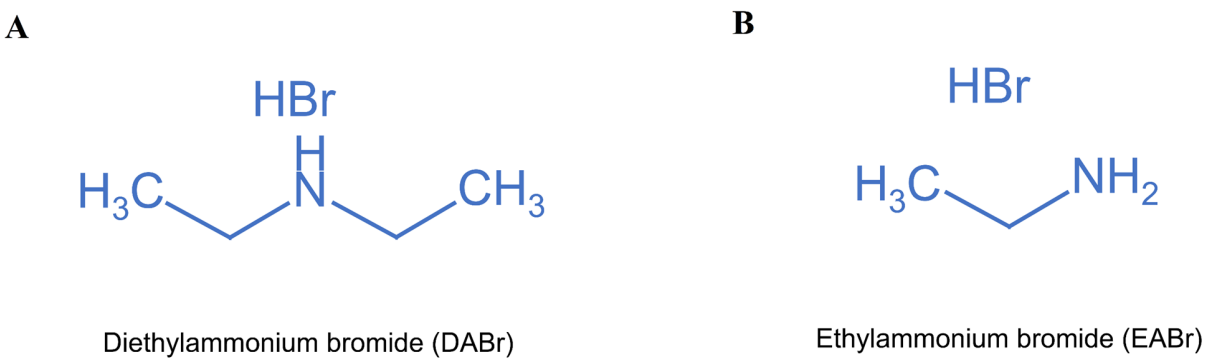

Fig. S1. Molecular structure. (A) Diethylammonium bromide and (B) Ethylammonium bromide.

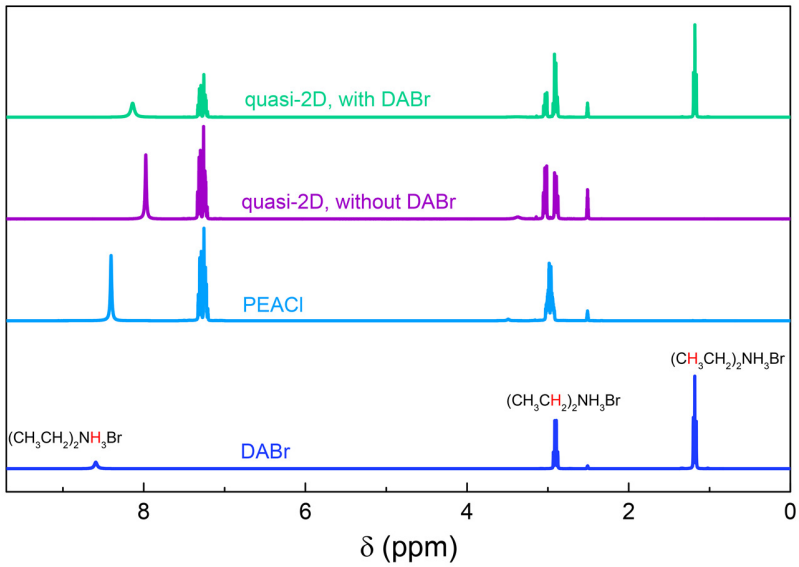

Fig. S2. ^{1}H NMR spectra of the DABr, PEACl powers and quasi-2D perovskite films with or without DABr.

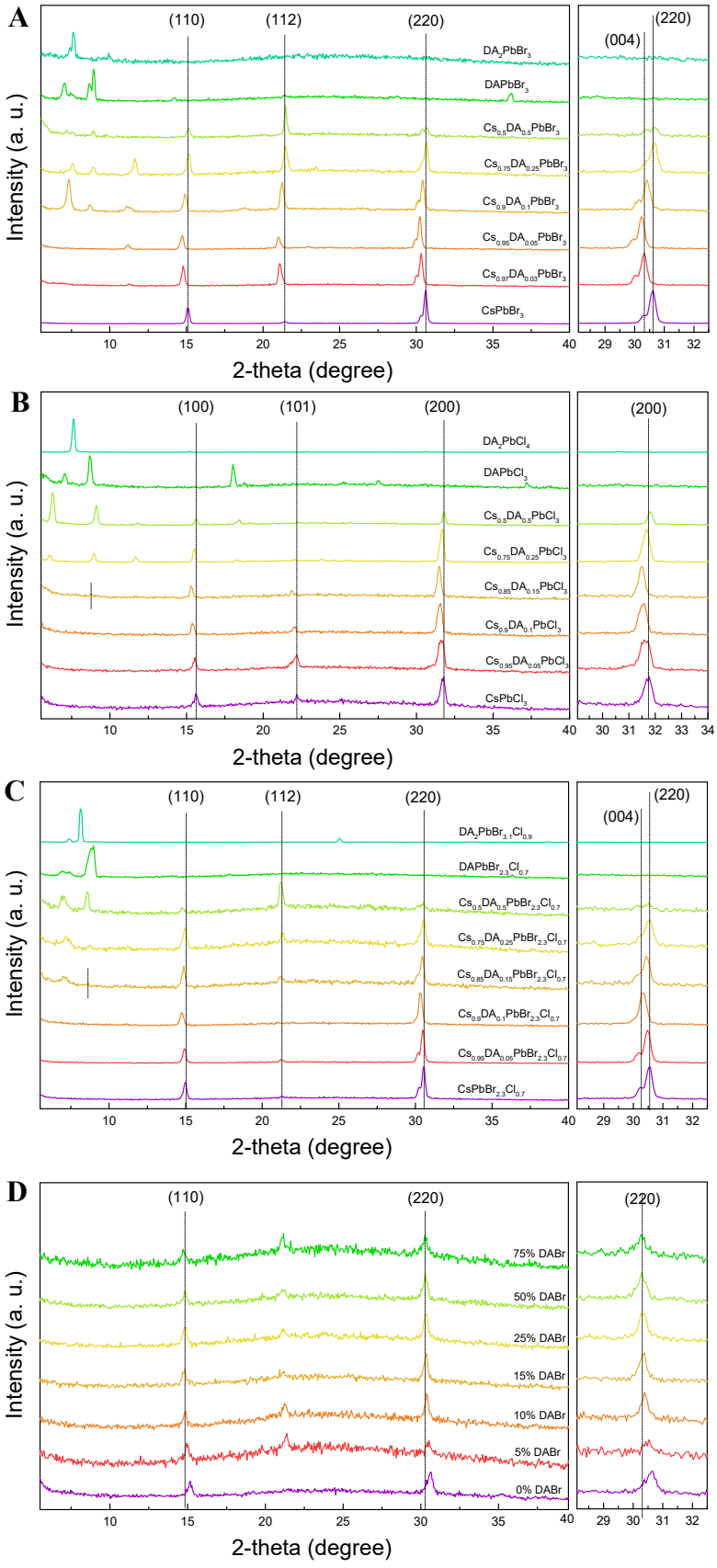

Fig. S3. XRD spectra of 3D and quasi-2D perovskites with different DA content. (A) $CsPbBr_3$, (B) $CsPbCl_3$, (C) $CsPbBr_{2.3}Cl_{0.7}$, and (D) PEA-$Cs_xDA_{1-x}PbBr_{2.3}Cl_{0.7}$.

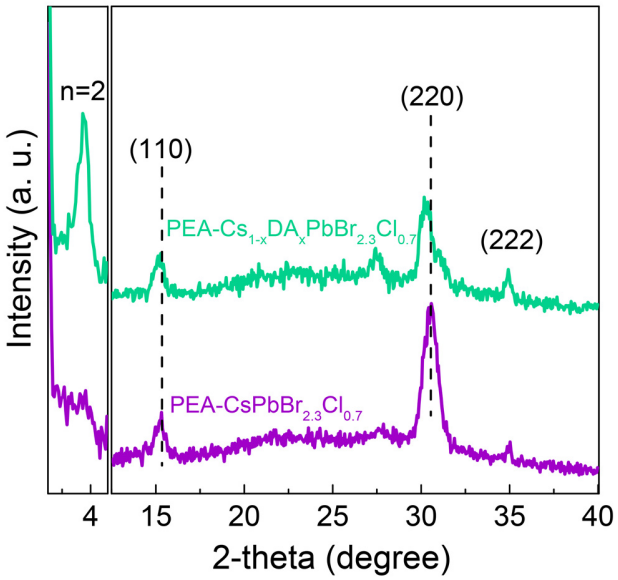

Fig. S4. XRD spectra of quasi-2D perovskite with and without DABr.

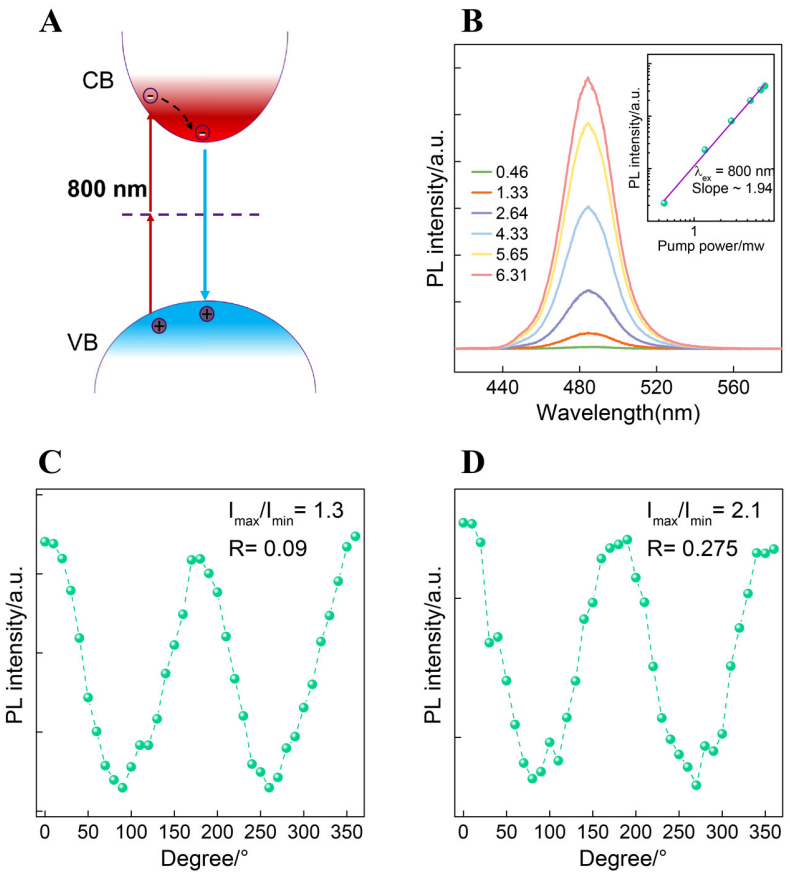

Fig. S5. The pumping fluence-dependent two-photon photoluminescence. (**A**) Schematic diagram of two-photon photoluminescence**.** (**B**) Two-photon excited PL spectra of PEA-$Cs_{1-x}DA_xPbBr_{2.3}Cl_{0.7}$, insets are plots of PL intensity versus optical intensity. (**C**) Two-photon excited PL intensity of PEA-$Cs_{1-x}DA_xPbBr_{2.3}Cl_{0.7}$ as a function of polarization angle of excitation light. (**D**) Two-photon PL intensity of PEA-$CsPbBr_{2.3}Cl_{0.7}$ measured by changing the rotation angle of the analyzer plate placed on the collection channel of the PL spectrometer.

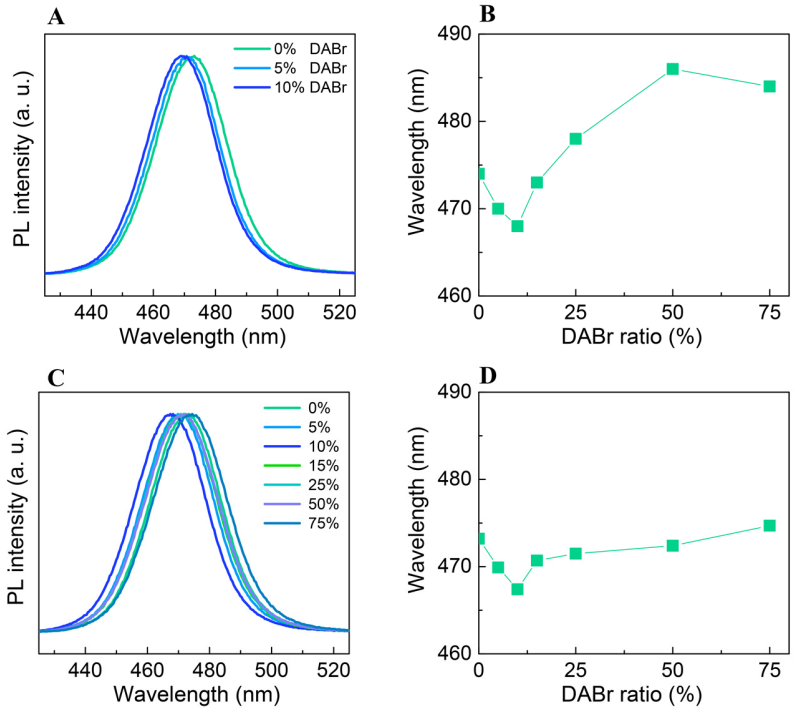

Fig. S6. PL spectra and peak shift of quasi-2D perovskite. (A) PL spectra and (B) PL peak position of PEA-$Cs_xDA_{1-x}PbBr_{2.3}Cl_{0.7}$ perovskite films with different DABr content. (C) PL spectra and (D) PL peak position of PEA-$Cs_xDA_{1-x}PbBr_{2.3}Cl_{0.7}$ perovskite films with different DABr:DACl content. Here DABr:DACl is used to replace DABr, and DABr/DACl ratio is kept at 3:1 to keep constant of the Br/Cl ratio in the perovskite.

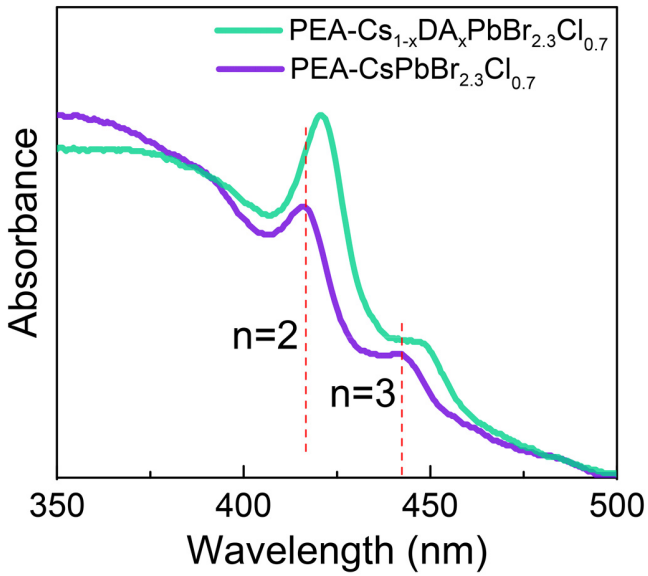

Fig. S7. UV-Vis absorption spectra of PEA-$Cs_{1-x}DA_xPbBr_{2.3}Cl_{0.7}$ and PEA-$CsPbBr_{2.3}Cl_{0.7}$ perovskite films.

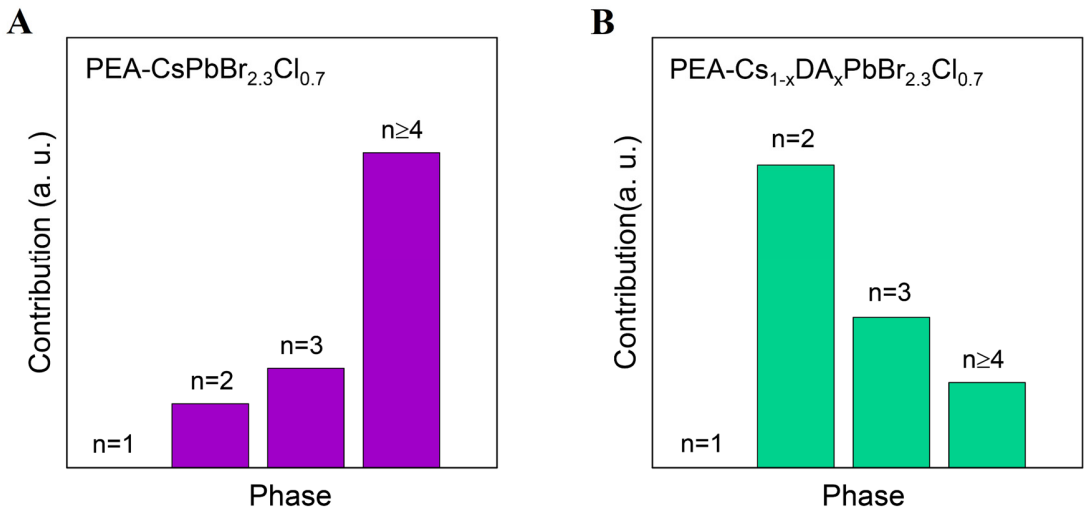

Fig. S8. Phase distribution. (A) PEA-$CsPbBr_{2.3}Cl_{0.7}$ and (B) PEA-$Cs_{1-x}DA_xPbBr_{2.3}Cl_{0.7}$ perovskite films. The relative contents of different phases were obtained according to the amplitude of GSB in TA spectra at 1 ps.

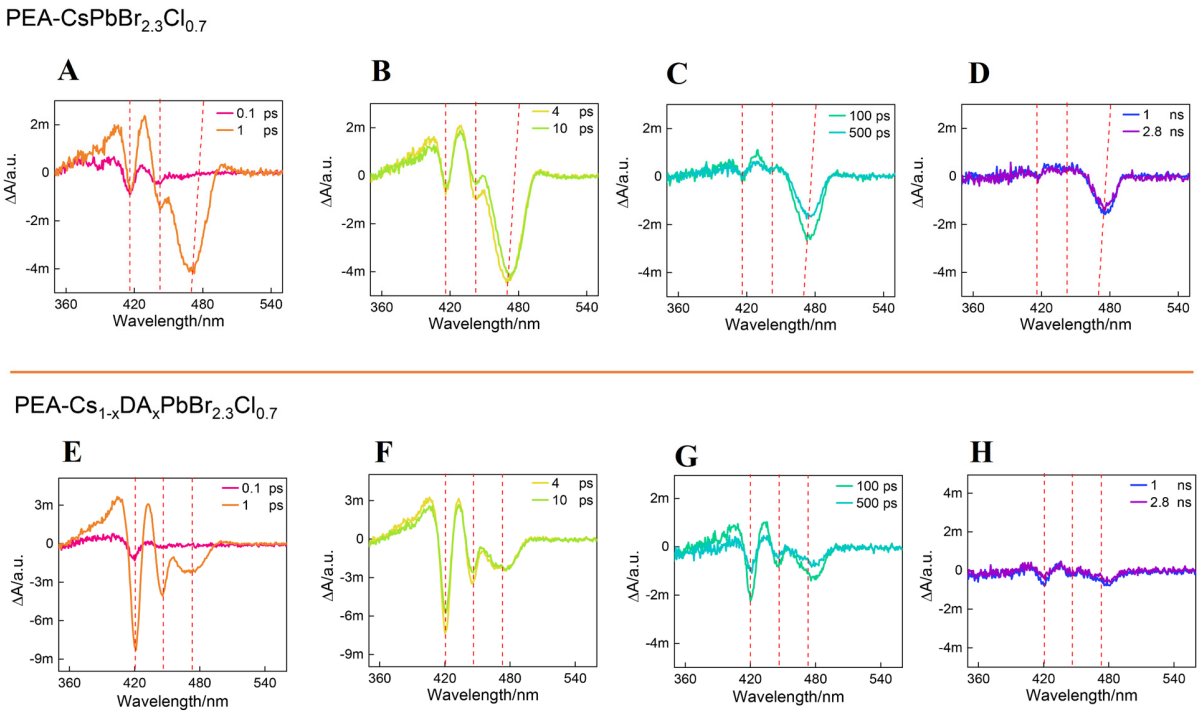

Fig. S9. The TA spectra at different timescale. (A-D) PEA-$CsPbBr_{2.3}Cl_{0.7}$;(E-H) PEA-$Cs_{1-x}DA_xPbBr_{2.3}Cl_{0.7}$

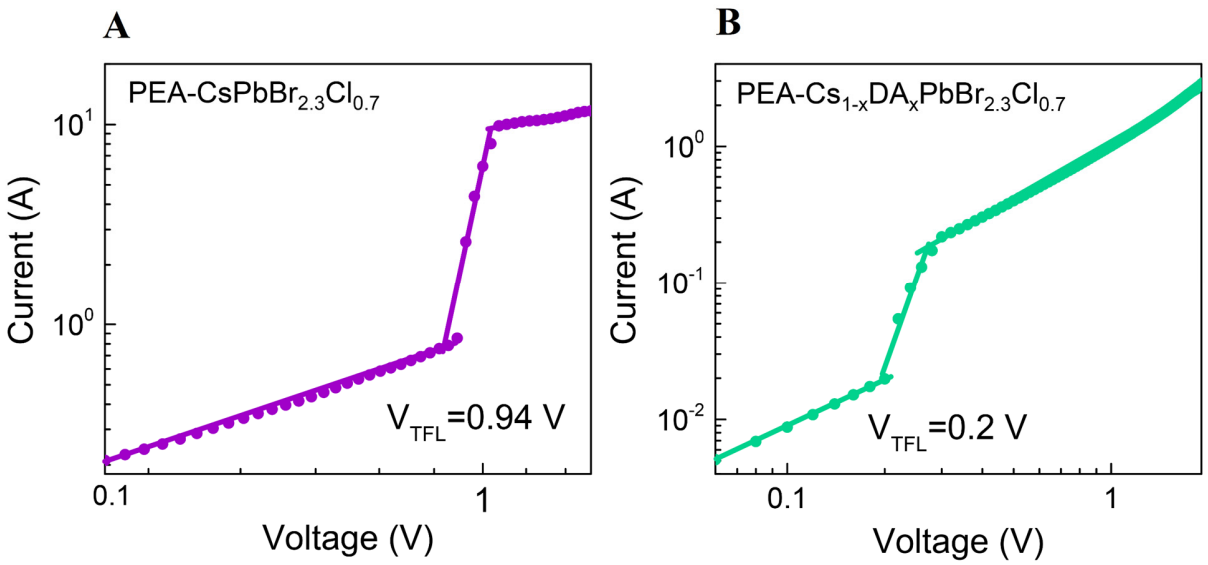

Fig. S10. The SCLC measurement. (A) PEA-$CsPbBr_{2.3}Cl_{0.7}$ and (B) PEA-$Cs_{1-x}DA_xPbBr_{2.3}Cl_{0.7}$. A hole-only device structure of ITO/PEDOT:PSS/perovskite/spiro-OMeTAD/Al was used to measure the space-charge-limited current (SCLC). The spiro-OMeTAD layer was spin-coated at 3000 r/min for 100 s without annealing. The rest of the preparation process is the same as in the main text. From the SCLC measurement, the parametric trap filled limit voltage (V_{TFL}) was estimated according to the transition from the linear to the nonlinear region.The defect state density (N_t) is determined by the formula: $N_t = 2V_{TFL}\cdot\varepsilon\varepsilon_0/eL^2$, where L is the thickness of the perovskite emissive layer, e is the is the elementary charge of the electron, ε is the relative permittivity, and ε_0 is the vacuum permittivity. The V_{TFL} decreases from 0.94 V (PEA-$CsPbBr_{2.3}Cl_{0.7}$) to 0.2 V (PEA-$Cs_xDA_{1-x}PbBr_{2.3}Cl_{0.7}$). Accordingly, N_t decreases from 4.14×10^{16} cm^{-3} to 8.8×10^{15} cm^{-3}.

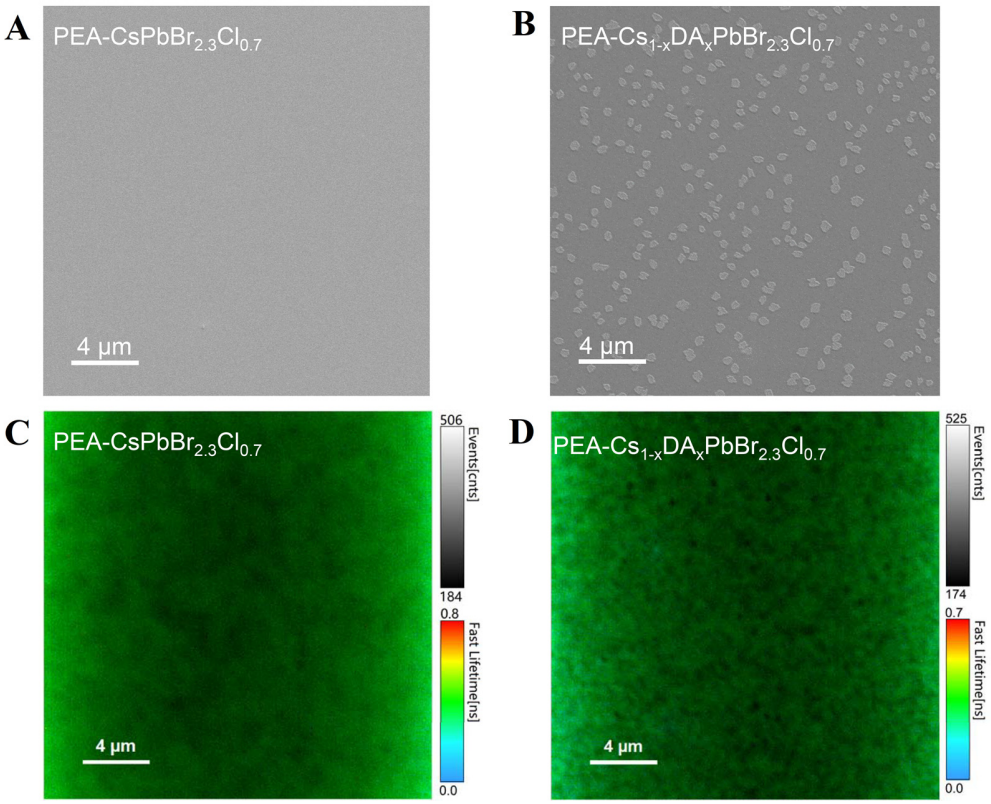

Fig. S11. Morphological properties of perovskite films. (**A-B**) SEM images and (**C-D**) fluorescence life time imaging microscopy images of PEA-$CsPbBr_{2.3}Cl_{0.7}$ and PEA-$Cs_{1-x}DA_xPbBr_{2.3}Cl_{0.7}$ films.

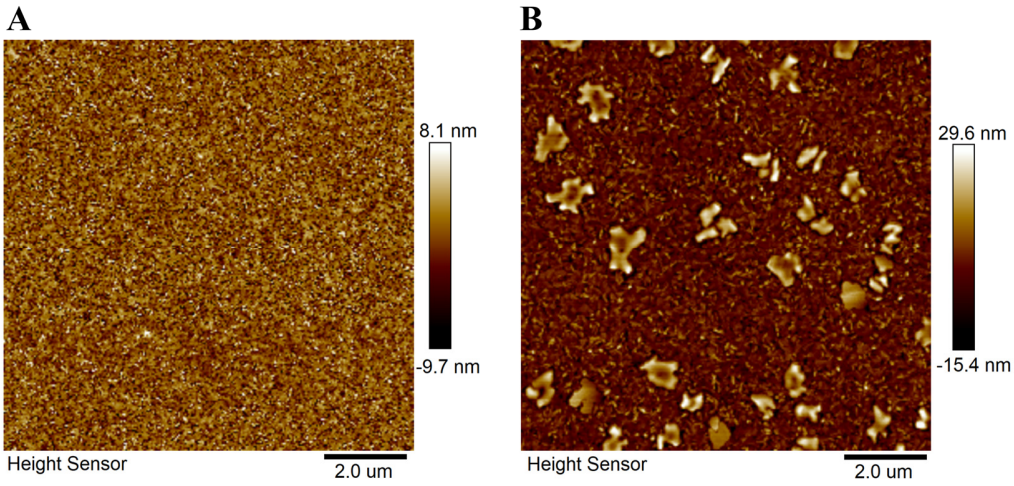

Fig. S12. AFM images. (A) PEA-$CsPbBr_{2.3}Cl_{0.7}$ and (B) PEA-$Cs_xDA_{1-x}PbBr_{2.3}Cl_{0.7}$ perovskite films.

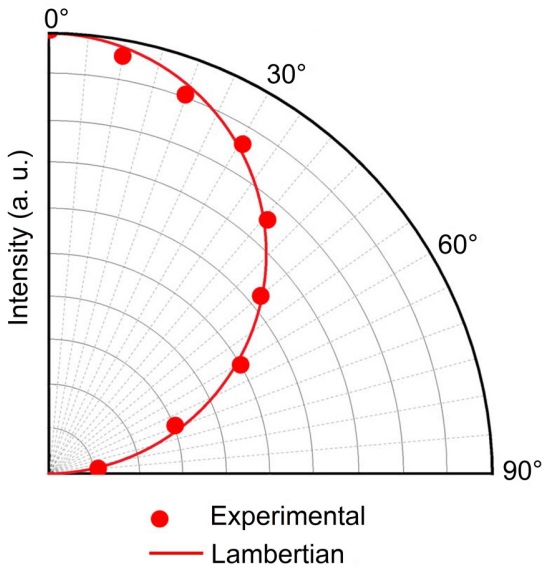

Fig. S13. Angle-dependent EL intensity of PeLEDs with PEA-$Cs_xDA_{1-x}PbBr_{2.3}Cl_{0.7}$ emitter.

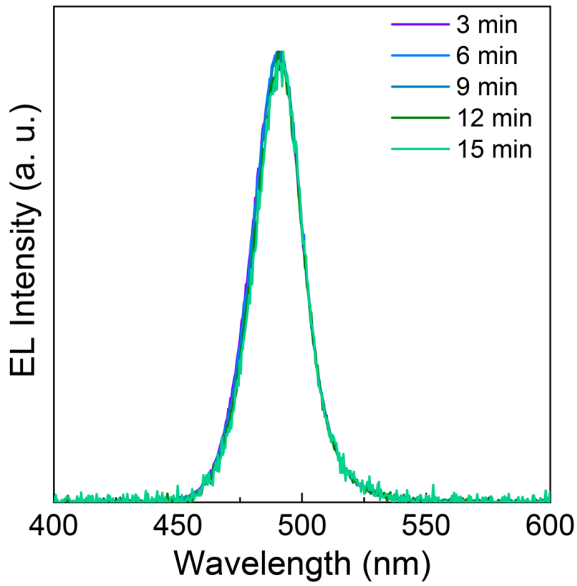

Fig. S14. Variation of EL spectrum under continuous operation.

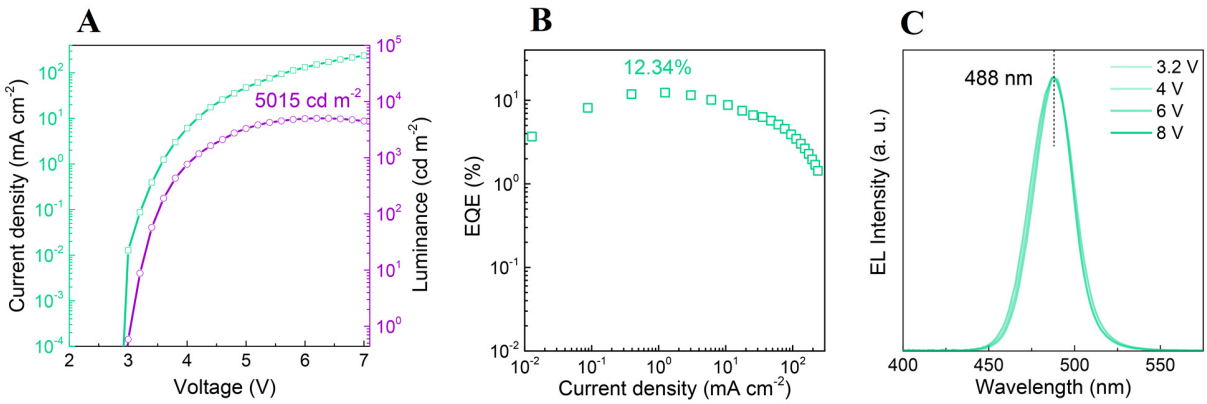

Fig. S15. The PeLED device performance with PEA-$Cs_{1-x}DA_xPbBr_{2.3}Cl_{0.7}$ perovskite emitter. (**A**) current density–luminance–voltage characteristics. (**B**) EQE characteristics. (**C**) the EL spectra at different biases.

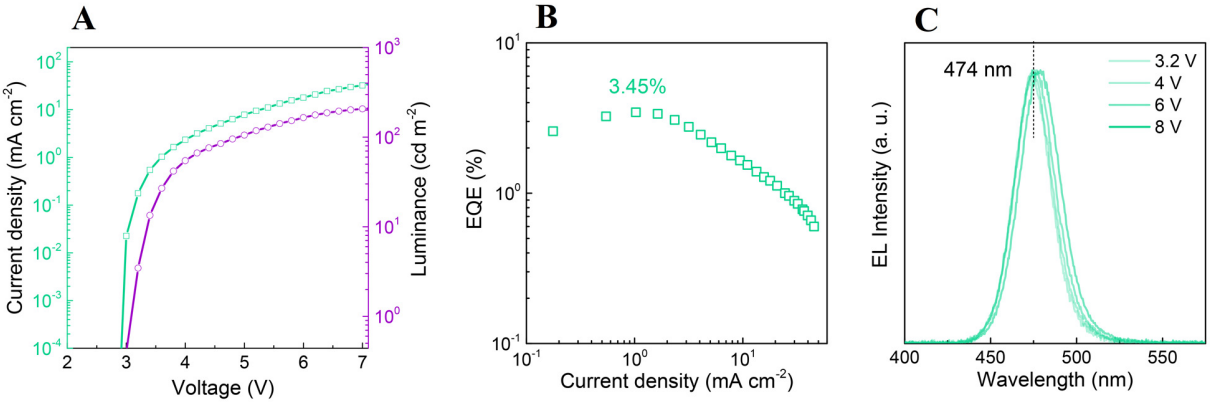

Fig. S16. The PeLED device performance with PEA-$CsPbBr_{2.3}Cl_{0.7}$ perovskite emitter. (**A**) current density–luminance–voltage characteristics. (**B**) EQE characteristics. (**C**) the EL spectra at different biases.

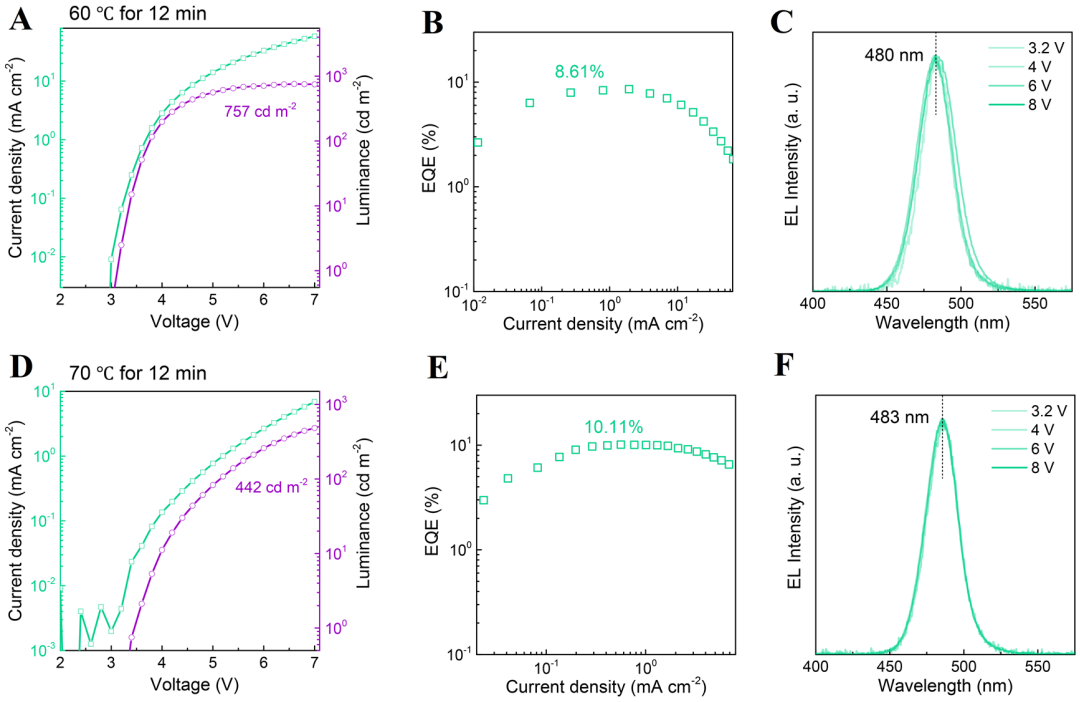

Fig. S17. The PeLED device performance with PEA-$Cs_{1-x}DA_xPbBr_{2.3}Cl_{0.7}$ perovskite emitter post-annealed at 60 ℃ and 70 ℃, respectively. (**A**), (**D**) current density–luminance–voltage characteristics. (**B**), (**E**) EQE characteristics. (**C**), (**F**) the EL spectra at different biases.

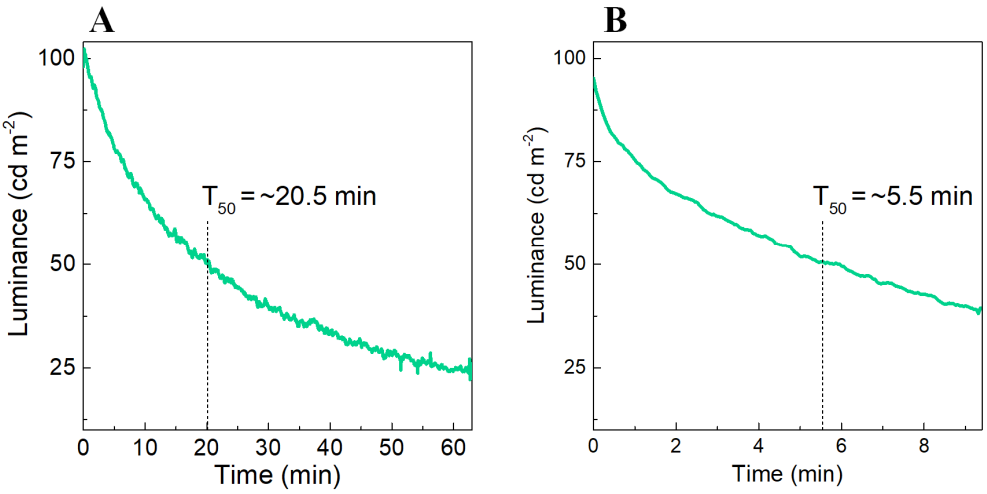

Fig. S18. The PeLED device's T_{50} at 100 cd m^{-2}. (A) PEA-$Cs_xDA_{1-x}PbBr_{2.3}Cl_{0.7}$ and **(B)** PEA-$CsPbBr_{2.3}Cl_{0.7}$ emitter.

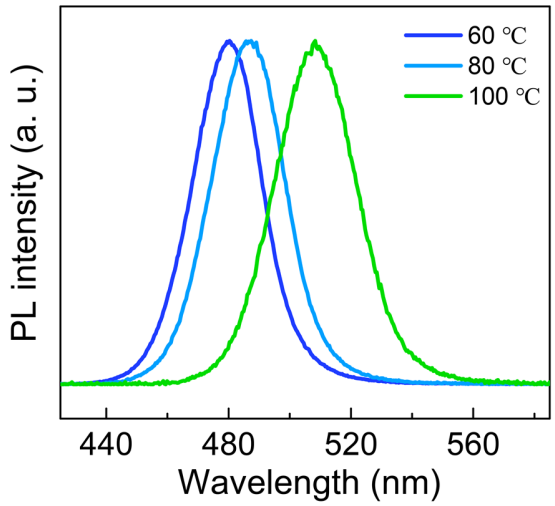

Fig. S19. PL spectra of PEA-$Cs_xDA_{1-x}PbBr_{2.3}Cl_{0.7}$ perovskite films post-annealed at different temperatures. The annealing temperature is 60°, 80°, 100°, respectively.

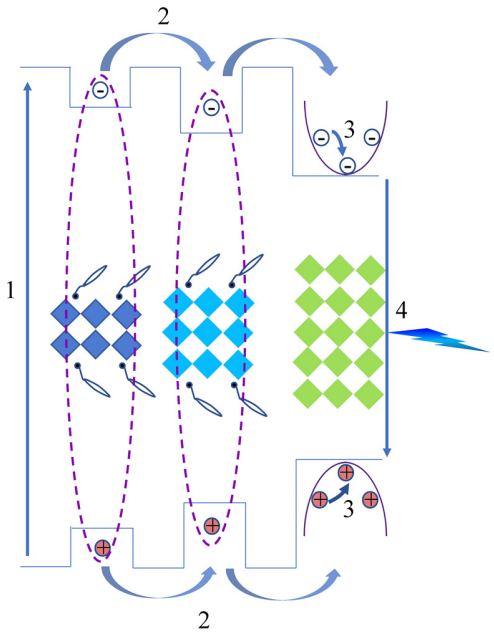

Fig. S20. Schematic carrier dynamic in a quasi-2D blue perovskite emitter.

Supplementary Note 1.
During DFT calculation, the cell is made of numbers of $CsPbBr_2Cl$ octahedra. The $CsPbBr_2Cl$ octahedra are also the main components responsible for the radiative/nonradiative recombination in the of the quasi-2D perovskite. Therefore, the theoretical predication of the excited-state transition of the 3D $CsPbBr_2Cl$ can be applicable to the quasi-2D perovskite.

Supplementary Note 2.
Recent studies have proven that a combination of large A-site cations (GA, EA, and DMA) balanced by small Cs cation could be employed to expand the lattice structure (ACS Energy Lett. 2018, 3, 6, 1261–1268; Nat Commun. 2020. 11. 4165; Adv. Funct. Mater. 2021, 2106691; ACS Energy Lett. 2020, 5, 1856−1864;). During the experiment, we find that DA insertion could lead to a similar tensile strain of +6% along lattice *a* direction, which fits well with the anticipation of the DFT simulation. More importantly, adding more DA cation addition in the quasi-2D perovskite will not lead more lattice distortion. In the case of EA with small radius, lattice expansion process will not stop when continuously increasing the EA concentration (Nat Commun. 2020. 11. 4165), and excessive lattice distortion may affect the stability of perovskite structure. This is different from DA in our case. In addition, DA has been used in perovskite solar cells and LEDs. It has been reported to change the film morphology, improve the crystallinity, and reduce the trap defects (Energy Environ. Sci., 2018, 11, 2353； Organic Electronics. 2019, 67,101–108； ACS Appl. Mater. Interfaces. 2020, 12, 14, 16707–16714). Based on the above considerations, we choose DA as the large cation in this work.

Supplementary Note 3.
$CsPbBr_3$ and $CsPbCl_3$ have energy bandgap (Eg) of 2.38 eV and 3.03 eV, respectively. the Eg of mixed halide perovskite can be estimated according to Vegard's Law:
Eg (eV) =2.38*(1-x) eV+3.03*x eV

where x is the Cl/Br ratio.
when adding PEABr in $CsPbBr_3$, emission peak shifts to 503 nm (2.465 eV). The emission peak shifts to 474 nm (2.616 eV) when adding the same amount of PEACl into $CsPbBr_3$. The variation of the bandgap is 151 meV, which is induced by Cl mixing. Thus, the Cl/Br ratio can be estimated to be 0.233 eV, corresponding to a composition of PEA-$CsPbBr_{2.3}Cl_{0.7}$.

Table S1. Cell parameters of the PEA-$CsPbBr_{2.3}Cl_{0.7}$ and PEA-$Cs_{1-x}DA_xPbBr_{2.3}Cl_{0.7}$. Rietveld Refinement method is used to derive the cell parameters. a,b,c are the lattice constant, V is the volume.

Cell parameter	**a**	**b**	**c**	**V**
PEA-$CsPbBr_{2.3}Cl_{0.7}$	7.504	9.508	11.687	833.844
PEA-$Cs_{1-x}DA_xPbBr_{2.3}Cl_{0.7}$	7.958	8.858	11.897	838.643
Delta[%]	6.0	-6.8	1.8	0.5

Table S2. Fitting parameters of the TA kinetics. The kinetics are fit by a multiple-exponential function: $\Delta A(t)=a_1\exp(-t/\tau_1)+ a_2\exp(-t/\tau_2)+ a_3\exp(-t/\tau_3)-c_1\exp(-t/\tau_{et})$, where a_1, a_2, a_3 and c_1 are the amplitudes and τ_1, τ_2, τ_3 are the decay time constants, τ_{et} is the formation time constant.

		τ_1 /ps (a_1)	τ_2 /ps (a_2)	τ_3 /ps (a_3)	τ_{et} /ps (c_1)
PEA-$CsPbBr_{2.3}Cl_{0.7}$	n=2	0.11 ps (49.3%)	2.13 ps (51.7%)		
	n=3	0.32 ps (42.5%)	2.08 ps (30.2%)	44.70 ps (28.3%)	
	n≥4	1.86 ps (18.1%)	64.7 ps (34.5%)	4713 ps (47.4%)	1.42 ps (28.2%)
PEA-$Cs_{1-x}DA_xPbBr_{2.3}Cl_{0.7}$	n=2	0.34 ps (18.8%)	3.42 ps (20.4%)	49.06 (60.8%)	
	n=3	0.36 ps (23.5%)	6.27 ps (32%)	63.50 ps (47.5%)	
	n≥4	0.62 ps (14.0%)	70.40 ps (52.9%)	2790 ps (37.2%)	0.77 ps (9.5%)